ASPS Conference Proceedings 1: 1495-1504 (2022)

Proceedings of

12th Structural Engineering Convention-An International Event (SEC 2022)

Available at https://asps-journals.com/index.php/acp

Investigation of Variable Wind Loads and Shape Accuracy of Reflectors in Parabolic Trough Collector

Natraj [1], K.S. Reddy [2, *], B.N. Rao [3]

[1] Department of Mechanical Engineering, Indian Institute of Technology, Madras, India
[2] Department of Mechanical Engineering, Professor, Indian Institute of Technology, Madras, India
[3] Department of Civil Engineering, Professor, Indian Institute of Technology, Madras, India

Paper ID - 140388

Abstract

Concentrated solar power is the technology involving reflectors which reflects the solar radiation and concentrates the radiations onto a receiver which absorbs the solar radiation and rises the temperature of the fluid flowing through it and the fluid is further used for process heating or power generation. Solar parabolic trough is the most established technology among the concentrated solar power technologies. For the optimization of the technology it is important to optimize the parabolic trough collectors from structural point of view as even gravity load is observed to cause a substantial effect on the shape of the reflector. Shape accuracy of the reflector is measured in terms of slope deviation. The slope deviation induced due to gravity and wind loads causes a change in optical and thermal efficiencies. The paper presents the study on pressure distribution at the surface of parabolic trough collector under different wind velocity, angle of attack of wind and orientation of the trough. Further, the pressure values over the trough surface are used to estimate the shape errors for the surface of the trough

Keywords: Concentrated solar power, parabolic trough collector, wind engineering, structural analysis.

1. Introduction

Solar energy has emerged as an important source of renewable energy. For the utilization of solar energy Concentrated solar power (CSP) is one of the matured technologies involving concentration of the solar radiation at a receiver which is further used for the power generation or process heating. Concentrated solar power has four major technologies which are parabolic trough collectors, parabolic dishes, solar towers and Linear Fresnel's, among which parabolic trough collectors is widely used technology in the solar power plants [1]. Parabolic trough collectors consist of parabolic shaped reflectors which concentrates the solar radiation at the receiver and even slight misalignment or decrease in shape quality of reflector causes a substantial decrease in the optical and thermal efficiencies of the collectors [2]. Shape error or slope deviation is the angle between the normal vectors of deformed surface and undeformed surface of the trough. Shape error is a measure to evaluate the shape accuracy of the reflectors. Due to heavy structural components and their movement to track the sun in different orientations, the deformations are mainly caused due to self-weight and wind loads [3]. Hence, it is important to evaluate displacements over the surface of parabolic trough collectors caused due to gravity and wind loads under different orientation of the trough collector. Since the wind flow is not always uniform over the trough surface, it is important to evaluate the pressure distribution over the surface of the trough due to non uniform wind loads to further assess the shape error caused due to such loads. To understand the pressure distribution over the surface of the trough two dimensional numerical study for the 250 kW solar power plant of parabolic trough collector located at Shiraz, Iran for collector angle of 90° to -90° in step of 30° and velocity 2.5 m/s to 15 m/s indicates that the maximum wind load on reflector and structural support occurs at 90° and minimum at 0° [4]. The parabolic trough collectors are subjected to wind loads as they are located in open terrain affecting tracking and convective heat transfer ability at

*Corresponding author. Tel: +914422574702; E-mail address: ksreddy@iitm.ac.in

Published online: December 19, 2022
doi:10.38208/acp.v1.681

the receiver. Numerical simulation for drag and lift force at a Reynolds number $Re_w = 3.6 \times 10^5$ for pitch angles 0° to 270° in step of 45° indicates that the maximum drag force occurs at 0° and decreases as the collector is moved to horizontal position 90° and lift force decreases from 90° to 0° and maximum lift force occurs at 60° [5]. Similar values of aerodynamic coefficient are obtained with a different numerical technique such as lattice Boltzmann for a standalone collector to study the wind behavior over a collector [6]. Study of wind load effects for different depth of trough, yaw angle and pitch angle show that the deeper troughs reduces the heat losses due to sheltering effect and wind loads decreases with the increase in yaw angle [7]. Uniform wind loads along with gravity loads are considered for the structural analysis and evaluation of the shape error in case of parabolic trough collector for 5.77 m aperture trough with length 4 m and an alternative composite material is found to have better performance than the conventional trough [8]. Experimental studies have also been conducted over the parabolic trough collector to study the wind behavior around the trough collector such as for wind load and pressure distribution on a 7.9 m section of aperture and width 5 m having a clearance of 0.35 m conducted using force balances and multi pressure acquisition system shows that most of the high pressure region occurs at the edge of the reflector due to vortex formation causing damage to the trough [9]. Field measurement for a 11.92 m long parabolic trough collector with aperture width of 5.76 m indicates maximum drag coefficient at 0° and 180° and minimum at 90°, also lift coefficient has maximum values at 60° [10]. Wind tunnel experiment for a scaled down model at 1:15 reveled that the high pressure are concentrated at the edges of the reflector where chances of breakage is more, hence improvement in stiffness at the edges of the reflector is suggested [11]. To quantify the effect of wind and gravity loads structural analysis for determining shape errors is carried under gravity load and values ~ 2 mrad are observed which is substantial compared to the measurements by Video Scanning Hartmann Optical Test (VSHOT) which is used to measure the shape error due to mounting methods, manufacturing errors and support contacts [12]. Under gravity load, shape errors are observed to change with orientation from 0° to 90° of the trough and shape errors are higher in elastic case involving brackets and mounting pad as the structural support than the stiff case with only mounting pads as the structural support [13]. Hence, study for finding aerodynamic coefficients and pressure distribution for the parabolic trough collector is done both numerically and experimentally but the corresponding wind loads has not been considered for the structural analysis of the parabolic trough collector instead uniform wind loads and gravity load alone has been considered. In this paper numerical analysis is carried out to find the distribution of pressure due to wind under different angle of attack and orientation of 5.77m aperture 4 m long trough. The non uniform wind load across the surface of the trough is then taken for the structural analysis to estimate the displacements and shape errors over the trough surface. Since, the structural components are the major cost incurred in the establishment of the solar power plants, it is important to optimize the parabolic trough collectors from a structural point of view and the present study will help in the design of lighter structures and optimization of the parabolic trough collector.

2. Pressure distribution over the trough

In this section wind flow analysis over the surface of trough is discussed. The wind load along with gravity load is then applied to the trough surface and analyzed for shape errors.

2.1 Numerical modeling and analysis for the wind flow

Numerical analysis is carried out to find the distribution of pressure due to wind under different angle of attack and orientation. To validate with Paetzold et.al [7], parabolic trough of aperture width of D= 5m is modeled. All the other dimensions are taken with reference to D. The material properties for air used in the fluid simulations are ρ=1.185 kg/m^3 and $\mu = 1.831 \times 10^{-5}$ kg/m s. Turbulence intensity is set to 5% at inlet and velocity 10 m/s. Shear Stress Transport (SST) turbulence model is chosen for the current study for its extensive and reliable usage for parabolic trough collectors. Velocity is given as the boundary condition at inlet and gauge pressure of 0 at the outlet. No-slip condition is given at the bottom of the domain and the parabolic solar collector surface. Mesh independence study was conducted. For the parabolic trough of height 5 m and length of 4 m the domain of total length 90 m, width 10.5 m and height 40 m is considered such that the blockage ratio of the object falls below 3%. Trough with aperture size of 5 m and width 10 m with ground clearance of 5 m to validate results with Paetzold .et. al. Solution domain is as shown in the Fig. 1. Further, the parabolic trough collector of 5.77 m aperture of length 4 m is considered for the study with the same computational domain as the blockage ratio falls below 3%. The entrance length of 15 m is provided and the leeward length of 75 m for it to develop. Pressure, coefficient of lift and drag and tabulated for different orientation and yaw angle cases.

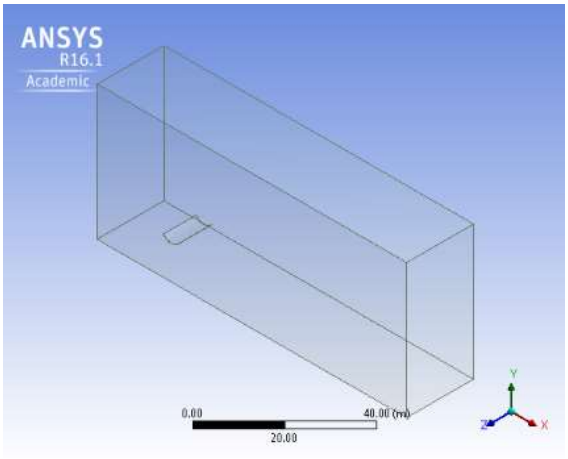

Fig. 1: Computational domain for a trough in 0-degree pitch angle

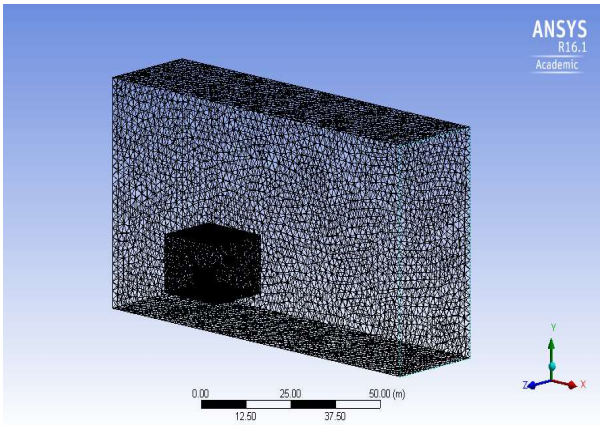

Fig. 2: Mesh generated for the study of pressure distribution

Mesh is generated separately and refined for each pitch case [5]. One more domain is enclosed around the PTC to improve the accuracy of the result. Tetrahedral cells of about 1,732,942 in number are generated in the domain. Computational domain and the mesh of the PTC is shown in Fig. 2 consisting of the two computational domain around the trough [15]. The analysis focuses on the wind force acting at the surface of the trough in the x and y direction, i.e. the drag and the lift force. The drag and lift coefficients C_d and C_l are plotted and compared for validation.

$$Cd = \frac{2FD}{\rho V^2{}_{ref} A}$$

$$Cl = \frac{2FL}{\rho V^2{}_{ref} A}$$

ρ is the air density (1.225 kg/m^3), A the characteristic area of the trough, i.e. aperture D times the width of the trough and is equal to 50 m^2 and V_{ref} is the velocity at reference height (10 m/s at 5 m height).

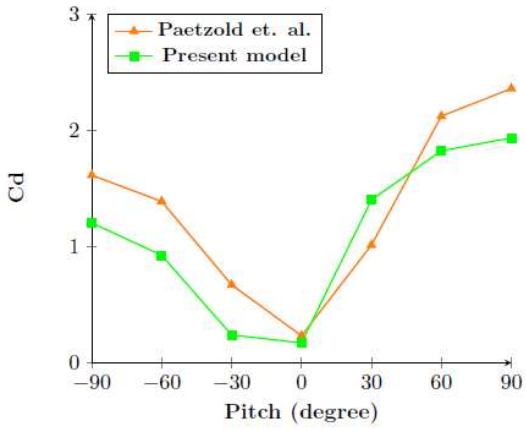

(a)

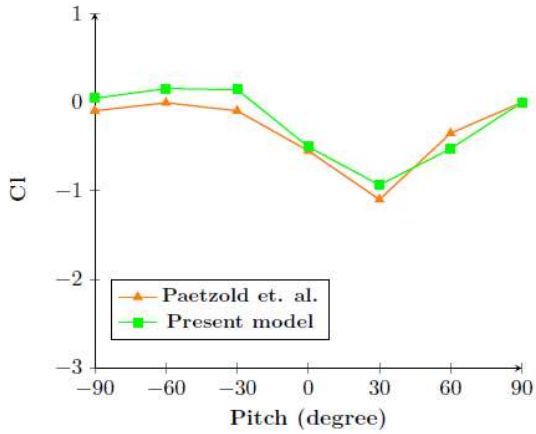

(b)

Fig 3: Validation with Paetzold et. al for (a) coefficient of drag C_d (b) coefficient of lift C_l

To validate with Paetzold et.al, parabolic trough aperture width of D= 5 m is modeled. All the other dimensions are taken with reference to D. Values agree well with the pressure and Cd, Cl values as obtained by Paetzold et. al. Convergence is obtained for residuals equals to 10^{-3}. Similarly, analysis is carried out for trough under pitch angles of -90°, -60°, -30°, 0°, 30°, 60°, 90°. There are regions of high pressure on the front side of the collector and regions of low pressure on the back or the leeward side of the reflector. Pressure values of 80.57 Pa for 90° and C_d and C_l values of 0.81 and -0.50 agrees well with the value of Paetzold et.al. Similarly, pressure, coefficient of lift and drag are obtained for the trough under pitch angles of -90°, -60°, -30°, 0°, 30°, 60°, 90°. Negative pressure values appear on the concave side of the trough in pitch angles of -90°, -60°, -30°. In -90° case values of -23 Pa and velocity close to 13.01 m/s are obtained.

2.2 Structural analysis for shape error in the trough

Based on the pressure distribution obtained from CFD results (Fig. 4), in postprocessing the values are averaged over each section (Fig. 5). Trough surface is divided in 12 sections and PTC with the surface of trough without division and with division is as shown in the Fig 7.

The analysis is carried for pitch angles 0°, 30°, 60°, 90° at three yaw angles 0°, 30°, 60° for each case. CFD analysis helps in finding the pressure distribution over the surface of the trough. Post processing of the results in MATLAB is done to find the pressure distribution over each section of the trough. Further, the pressure obtained over each section in CFD is applied as the load for structural analysis where displacement and slope deviations are calculated

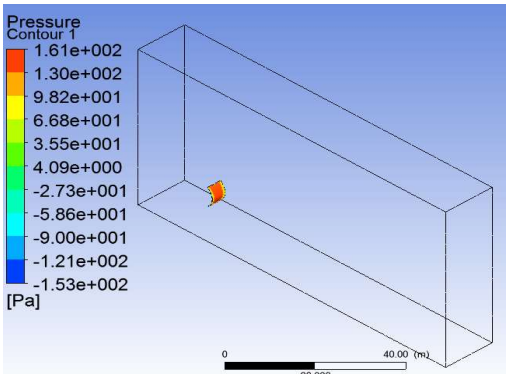

Fig. 4: Pressure distribution on the trough at 90° pitch angle

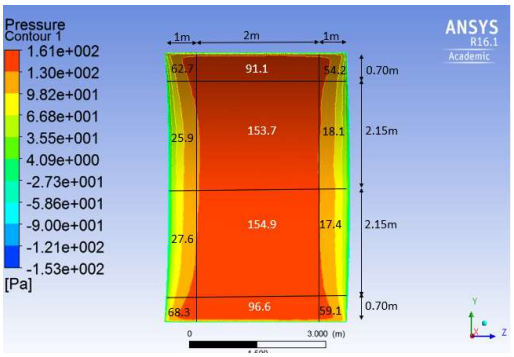

Fig 5: Pressure distribution over sections of the trough

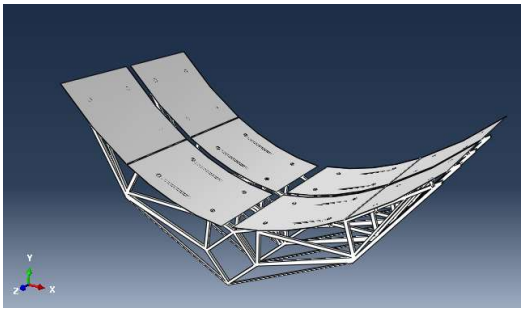

Fig 6: PTC without division of section

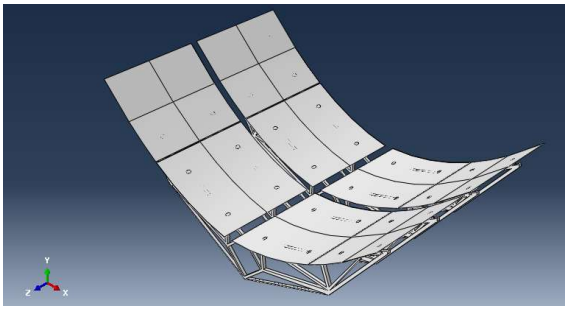

Fig 7: PTC with division of section

Glass is used as the trough material mounted on ceramic mounting pads and attached to support arm through alumunium brackets. Surface to surface interaction and tie constraint between the interacting surfaces are used. Fixed boundary condition is used at the rear end of the support arm at each orientation. A static stress analysis is used as the inertia effects can be neglected. Coefficient of pressure, Cp for each section is obtained using the formula as given below.

$$Cp = \frac{Pf - Pb}{{}^{1}/_{2}\,\rho v^2}$$

where P is the averaged pressure over each section and ρ is the density of air and v is the speed of wind. Displacements of the trough surface is obtained with structural analysis which is postprocessed for shape errors

FD equations

Conservation of mass $\frac{\partial \bar{u}_j}{\partial \bar{x}_j} = 0$

Conservation of momentum

$$\frac{\partial}{\partial x}(\rho \bar{u}_i \bar{u}_j) = -\frac{\partial P}{\partial x_i} + \frac{\partial}{\partial x_j}\left(\mu \frac{\partial \bar{u}_j}{\partial \bar{x}_j} - \rho \overline{u'_i u'_j}\right)$$

$$-\rho \overline{u'_i u'_j} = \mu_t \left(\frac{\partial \bar{u}_j}{\partial \bar{x}_i} + \frac{\partial \bar{u}_i}{\partial \bar{x}_j}\right) - \frac{2}{3}\rho \delta_{ij} k$$

$$\frac{\partial}{\partial x_j}(\rho \bar{u}_j \mathrm{k}) = \frac{\partial}{\partial x_j}\left(\left(\mu + \frac{\mu_t}{\sigma_{k2}}\right)\frac{\partial \mathrm{k}}{\partial \mathrm{x}_j}\right) + P_k - \beta^* \rho k \omega$$

$$\frac{\partial}{\partial x_j}(\rho \bar{u}_j \omega) = \frac{\partial}{\partial x_j}\left(\left(\mu + \frac{\mu_t}{\sigma_{k2}}\right)\frac{\partial \omega}{\partial \mathrm{x}_j}\right) + (1 - F_1) 2\rho \frac{1}{\sigma_{\omega_2} \omega} \frac{\partial k}{\partial \bar{x}_j} \frac{\partial \omega}{\partial \bar{x}_j} + \alpha_2 \frac{\omega}{k} P_k - \rho \beta_2 \omega^2$$

$$F_1 = \tanh(arg_1^4)$$

$$arg_1 = \min\left(max\left(\frac{\sqrt{k}}{\beta^* \omega y}\frac{500v}{\omega y^2}\right), \frac{4\rho k}{CD_{k\omega}\sigma_{\omega_2} y^2}\right)$$

$$CD_{k\omega} = \max\left(2\rho \frac{1}{\sigma_{\omega_2}\omega}\frac{\partial \mathrm{k}}{\partial \mathrm{x}_j}\frac{\partial \omega}{\partial \mathrm{x}_j}\ 1.0 \times 10^{-10}\right)$$

$$P_k = \mu_t\left(\frac{\partial \bar{u}_j}{\partial \bar{x}_i} + \frac{\partial \bar{u}_i}{\partial \bar{x}_j}\right)\frac{\partial \bar{u}_i}{\partial \bar{x}_j}$$

$$\mu_t = \frac{\rho a_1 k}{\max(a_1\omega, SF_2)}$$

$$F_2 = \tanh(arg_2^4)$$

$$arg_2 = max\left(\frac{2\sqrt{k}}{\beta^* \omega y}\frac{500v}{\omega y^2}\right)$$

3. Results and discussion

3.1. Glass trough at different pitch angles

The analysis gives the pressure distribution over both front and back surface of the trough. The trough is divided into different sections based on the pressure distribution as shown in Fig.7. The displacements over the surface of the glass trough subjected to gravity and wind loads at different orientation 0°, 30°, 60° and 90° is as shown in the Fig. 8. Maximum displacemets is observed at 30° and 60° orientation with values 1.64 and 1.67 mm respectively. Slope deviation or shape error is calculated by postprocessing the displacement values and it is observed to be maximum at 60° orientation with value of 1.72 mrad. Maximum displacements occurs at the edges of the mirror panels. The shape error increases with the orientation from 0° to 60° and decreases for 90°.

3.2. Glass trough at different yaw and pitch angles

The structural analysis is carried out for different angle of attack of wind called yaw angle. CFD analysis is carried out for 0°, 30°, 60° yaw angles for orientations 0°, 30°, 60°, 90° of the parabolic trough collectors. As seen in Table 1 the displacements decrease from 1.16 to 0.26 mm in case of 0° orientation with yaw angle change from 0° to 60° and shape error decreases from 1.22 to 0.99 mrad. The displacements on the reflectors for the parabolic trough collector under yaw angles of 30° and 60° for pitch angles 0°, 30°, 60° and 90° is shown in Fig. 9. The displacement values are further used to find the angle between the normal vectors of the deformed and undeformed trough surface which gives the shape accuracy of the trough also called as shape error or slope deviation and are tabulated in Table 2.

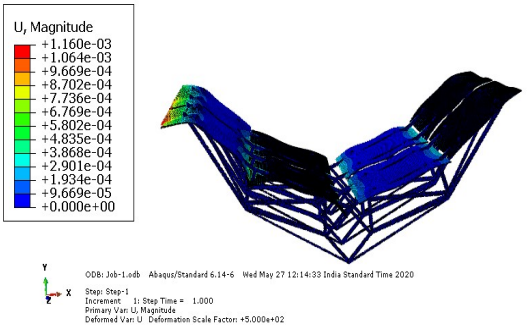

(a) 0° Pitch angle

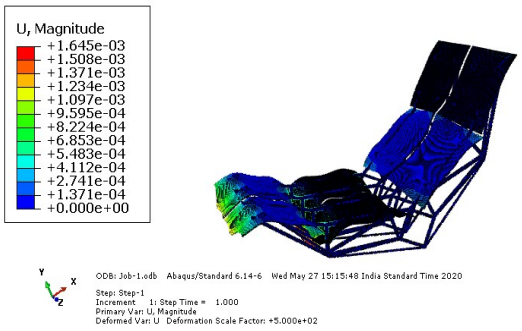

(b) 30° Pitch angle

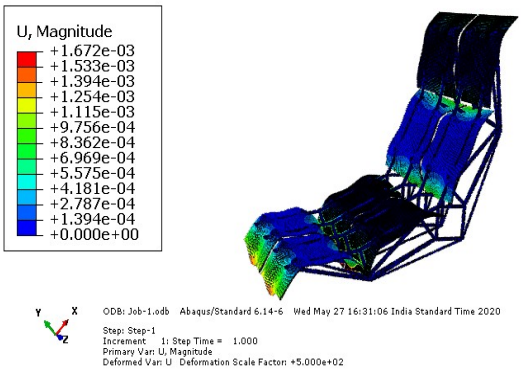

(c) 60° Pitch angle

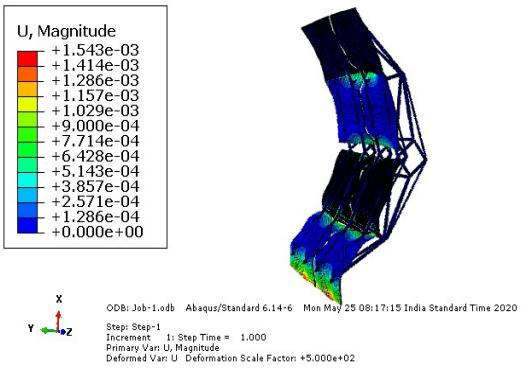

(d) 90° Pitch angle

Fig 8: Displacement over the trough under pitch angles of (a) 0° (b) 30° (c) 60° (d) 90°

Table 1: Displacement of the trough at yaw angles for different pitch angles

Pitch	Yaw	U(mm)
0°	0°	1.16
	30°	0.72
	60°	0.26
30°	0°	1.64
	30°	1.36
	60°	0.75
60°	0°	1.67
	30°	1.37
	60°	0.93
90°	0°	1.54
	30°	1.47
	60°	0.85

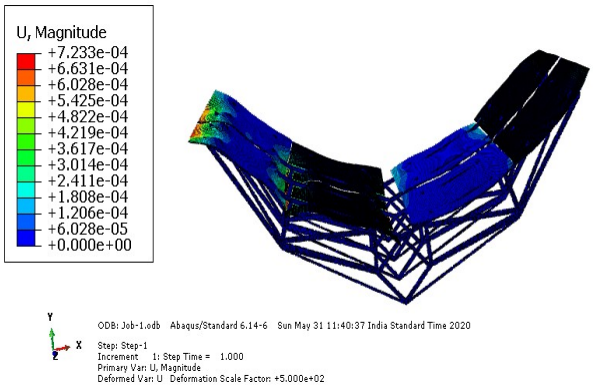

(a) Pitch 0° yaw 30°

(b)

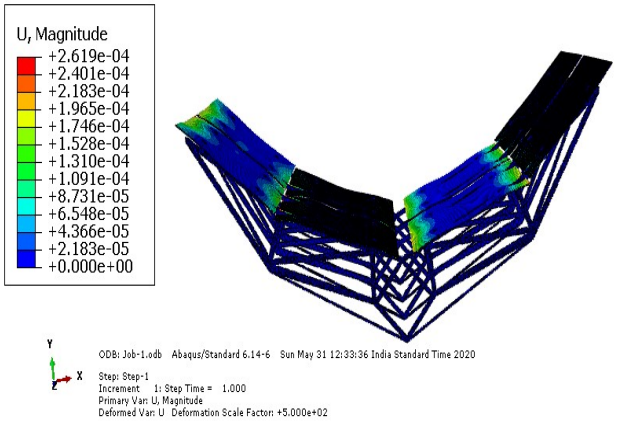

(c) Pitch 0° yaw 60°

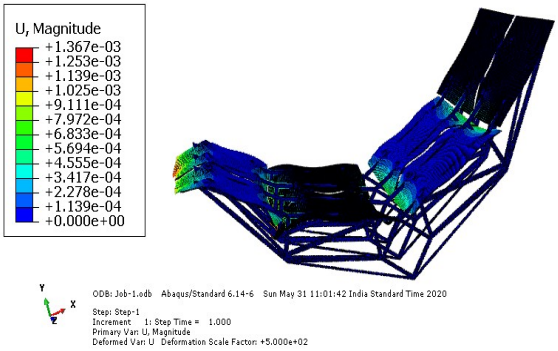

(d) Pitch 30° yaw 30°

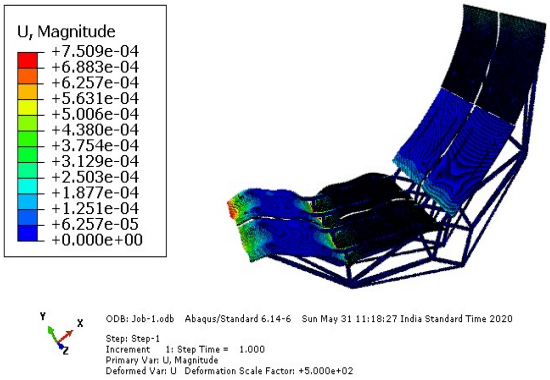

(e) Pitch 30° yaw 60°

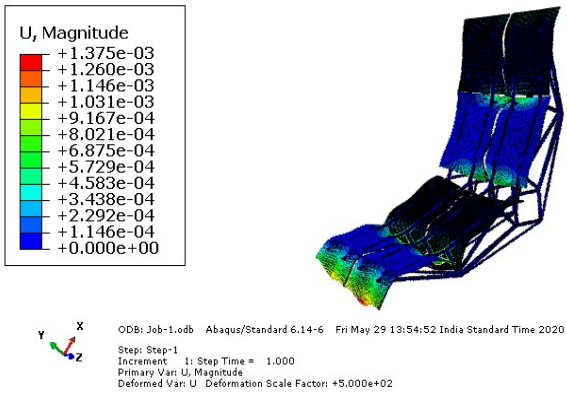

(f) Pitch 60° yaw 30°

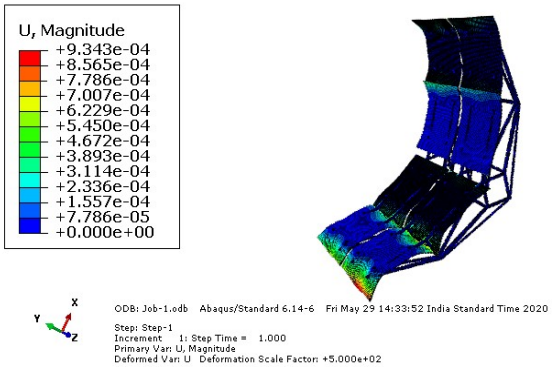

(g) Pitch 60° yaw 60°

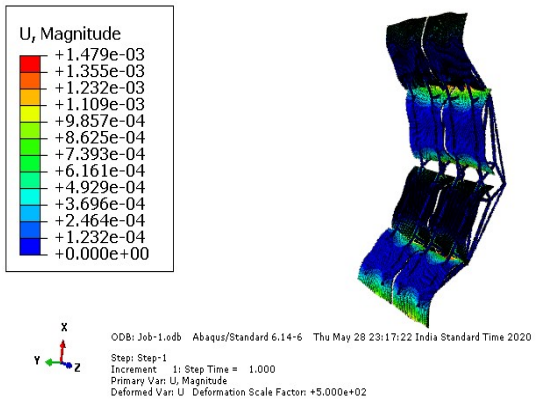

(h) Pitch 90° yaw 30°

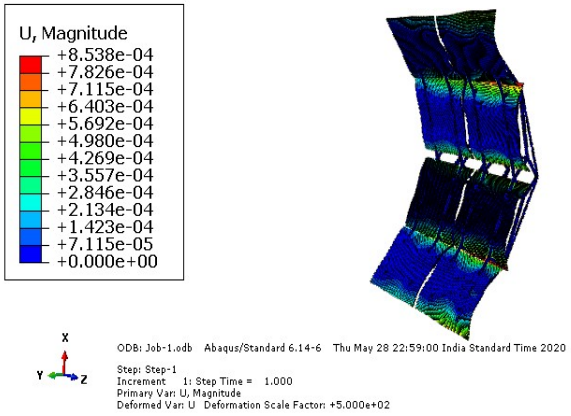

(i) Pitch 90° yaw 60°

Fig 9: Displacement over the surface of trough for yaw angles of 30°, 60° yaw angles for orientations 0°, 30°, 60°, 90°

Table 2: Shape error of the trough at yaw angles for different pitch angles

Pitch	Yaw	SD (mrad)
	0°	1.22
	30°	1.11
0°	60°	0.99
	0°	1.48
	30°	1.44
30°	60°	1.11
	0°	1.72
	30°	1.48
60°	60°	1.18
	0°	1.53
	30°	1.34
90°	60°	1.29

3.3. Aluminium trough at different pitch and yaw angle

Reflectors of the parabolic trough collector are made mostly of glass and aluminium material. Hence, analysis is also carried out for aluminium trough. Pressure distribution over the surface of the trough is estimated for aluminium trough and the values obtained through the analysis are averaged over the surface of the trough and given as input for the structural analysis. Trough surface is divided into different sections and wind loads are applied separately over each section over the trough surface. Table 3 shows displacement values which decrease with change in angle of attack from 0° to 30° in all the pitch angles of the trough. 1.64 mm and 1.67 mm are the maximum values of displacement at the surface of trough at 0° yaw angle for orientations 30° and 60° respectively. The displacement values at each node is postprocessed for both undeformed and deformed trough surface and equation of the plane using nodes is generated. Further, the angle between the normal vector of the deformed and undeformed trough surface gives the shape accuracy of the trough also called as shape error or slope deviation. Shape error values (Table 4) of 1.27 mrad is observed for aluminium trough against 1.22 mrad for a glass trough for 0° yaw angle at 0° orientation. Similarly, the shape error is observed to be greater than the glass trough case due to lesser stiffness of the material in all the pitch and yaw angle cases. Fig. 10 shows the displacement over the trough surface at different orientations 0°, 30°, 60°, 90°.

Table 3: Displacement of the aluminium trough at yaw angles for different pitch angles

Pitch	Yaw	U(mm)
0°	0°	1.18
	30°	0.73
	60°	0.30
30°	0°	1.64
	30°	1.37
	60°	0.80
60°	0°	1.66
	30°	1.37
	60°	0.98
90°	0°	1.52
	30°	1.19
	60°	1.11

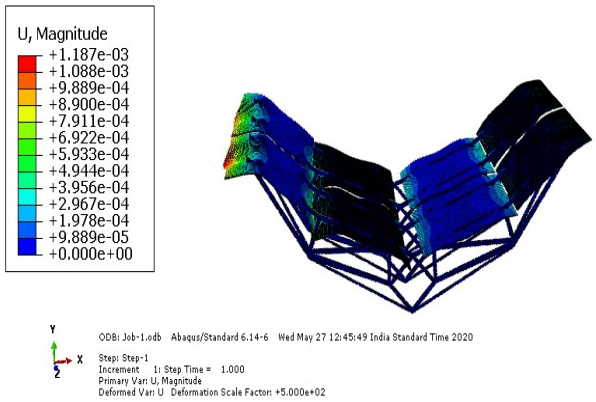

(a) 0° Pitch

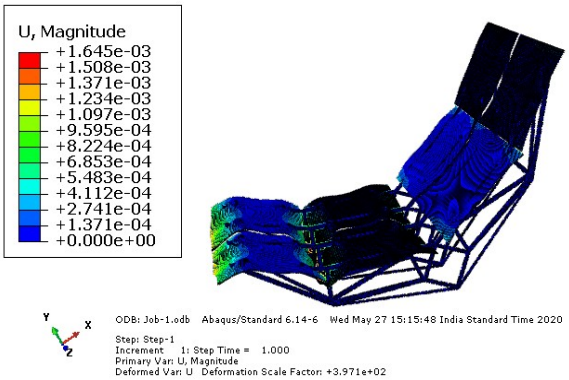

(b) 30° Pitch

(c) 60° Pitch

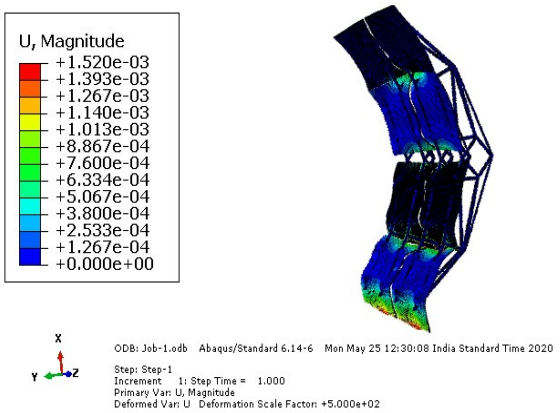

(d) 90° Pitch

Fig 10: Displacement over the trough under pitch angles of (a) 0° (b) 30° (c) 60° (d) 90°

The structural analysis is further carried out for different angle of attack. CFD analysis is carried out for 0°, 30°, 60° yaw angles for orientations 0°, 30°, 60°, 90° of the parabolic trough collectors with aluminium trough material. As seen in Table 3 the displacements decrease from 1.18 to 0.30 mm in case of 0° orientation with yaw angle change from 0° to 60° and shape error decreases from 1.27 to 1.02 mrad. The displacements on the reflectors for the parabolic trough collector under yaw angles of 30° and 60° for pitch angles 0° is shown in Fig. 11. Deformations under non uniform wind and gravity load are observed to be maximum at the edges of the mirror. The values of the displacements and slope deviation is observed to decrease with the yaw angle from 0° to 60°.

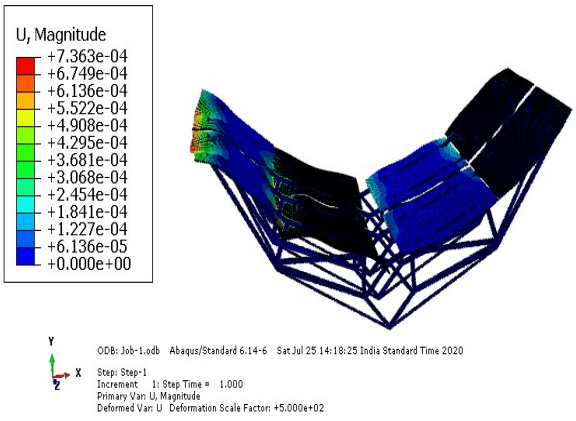

(a) Pitch 0° yaw 30°

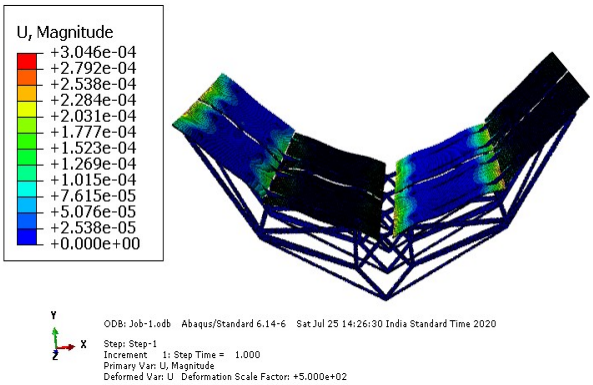

(b) Pitch 0° yaw 60°

Fig 11: Displacement over the surface of trough for yaw angles of 30°, 60° yaw angles for 0° orientation.

Table 4: Shape error of the trough at yaw angles for different pitch angles

Pitch	Yaw	SD (mrad)
0°	0°	1.27
	30°	1.12
	60°	1.02
30°	0°	1.49
	30°	1.47
	60°	1.14
60°	0°	1.73
	30°	1.50
	60°	1.20
90°	0°	1.52
	30°	1.37
	60°	1.23

4. Conclusions

The study is carried out to estimate the effect of wind and the gravity loads on the surface of parabolic reflectors. Pressure distribution over the surface of the reflectors is estimated at different orientations and angle of attack to understand the wind loads acting on the parabolic trough collectors. The reflector is then subjected to gravity load for structural analysis along with the wind loads obtained using CFD. Effect of gravity and wind load is quantified in terms of displacements over the trough surface and corresponding change in accuracy of shape of reflectors as shape errors. Shape errors as high as 1.72 and 1.53 mrad are obtained at 60° and 90° orientation respectively for glass trough at 0° yaw angle. Values of shape errors decrease with change in yaw angle from 0° to 60°. Shape errors are greater for Alumunium trough than the glass trough due to lesser stiffness of the material and also decrease with change in yaw angle for each orientation 0°, 30°, 60° and 90° of the troughs. Values of shape errors are observed to be maximum at 60° orientation. Hence, reflectors of the parabolic trough can be optimized for this orientation. Analysis will help in the design and optimization of parabolic trough collectors. Analyzing the effect of other parameters such as width of the trough, Reynolds number, depth of the trough, elevation and azimuth angle will be considered in the future work.

Acknowledgment

The financial support provided by Ministry of Human Resource and Development (MHRD), Government of India (Project code: P1374 under Scheme for Promotion of Academic and Research Collaboration (SPARC)) is duly acknowledged.

Disclosures

Free Access to this article is sponsored by SARL ALPHA CRISTO INDUSTRIAL.

References

[1] Bellos E, Tzivanidis C. Alternative designs of parabolic trough solar collectors. Prog Energy Combust Sci 2019;71:81–117.

[2] Moya EZ. Parabolic-trough concentrating solar power (CSP) systems. Conc Sol Power Technol 2012:197–239.

[3] Fu W, Yang MC, Zhu YZ, Yang L. The Wind-structure Interaction Analysis and Optimization of Parabolic Trough Collector. Energy Procedia 2015;69:77–83.

[4] Naeeni N, Yaghoubi M. Analysis of wind flow around a parabolic collector (1) fluid flow. Renew Energy 2007;32:1898–916.

[5] Hachicha AA, Rodríguez I, Castro J, Oliva A. Numerical simulation of wind flow around a parabolic trough solar collector. Appl Energy 2013;107:426–37.

[6] Andre M, Mier-Torrecilla M, Wüchner R. Numerical simulation of wind loads on a parabolic trough solar collector using lattice Boltzmann and finite element methods. J Wind Eng Ind Aerodyn 2015;146:185–94.

[7] Paetzold J, Cochard S, Fletcher DF, Vassallo A. Wind Engineering Analysis of Parabolic Trough Collectors to Optimise Wind Loads and Heat Loss. Energy Procedia 2015;69:168–77.

[8] Reddy KS, Singla H, Natraj. Gravity & wind load analysis and optical study of solar parabolic trough collector with composite facets using optimized modelling approach. Energy 2019;189:116065.

[9] Hosoya N, Peterka JA, Gee RC, Kearney D. Wind Tunnel Tests of Parabolic Trough Solar Collectors.

North 2008:133.

[10] Gong B, Wang Z, Li Z, Zhang J, Fu X. Field measurements of boundary layer wind characteristics and wind loads of a parabolic trough solar collector. Sol Energy 2012;86:1880–98.

[11] Zou Q, Li Z, Wu H, Kuang R, Hui Y. Wind pressure distribution on trough concentrator and fluctuating wind pressure characteristics. Sol Energy 2015;120:464–78.

[12] Christian JM, Ho CK. Finite Element Modeling and Ray Tracing of Parabolic Trough Collectors for evalution of optical intercept factors with gravity loads. Proc ASME 2011 5th Int Conf Energy Sustain 2011:1–9.

[13] Meiser S, Kleine-Büning C, Uhlig R, Lüpfert E, Schiricke B, Pitz-Paal R. Finite element modeling of parabolic trough mirror shape in different mirror angles. ASME 2012 6th Int Conf Energy Sustain ES 2012, 2012:429–35.

[14] Dittenber DB, Gangarao HVS. Composites : Part A Critical review of recent publications on use of natural composites in infrastructure. Compos Part A 2012;43:1419–29.

[15] Reddy KS, Veershetty G, Srihari Vikram T. Effect of wind speed and direction on convective heat losses from solar parabolic dish modified cavity receiver. Sol Energy 2016;131:183–98.